Supplement of Nonlin. Processes Geophys., 27, 261–275, 2020
https://doi.org/10.5194/npg-27-261-2020-supplement

Nonlinear Processes in Geophysics
Open Access
EGU

Supplement of

Detecting dynamical anomalies in time series from different palaeoclimate proxy archives using windowed recurrence network analysis

Jaqueline Lekscha and Reik V. Donner

Correspondence to: Jaqueline Lekscha (lekscha@pik-potsdam.de)

Additional figures

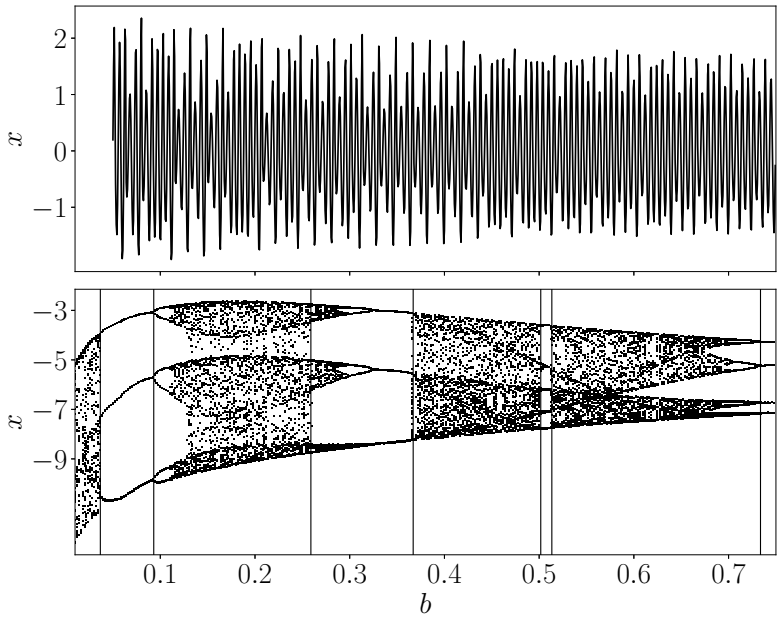

Figure S1. Transient time series of the x-component of the Rössler system with parameter b varying in every integration step (top) and Feigenbaum diagram for corresponding stationary system (bottom).

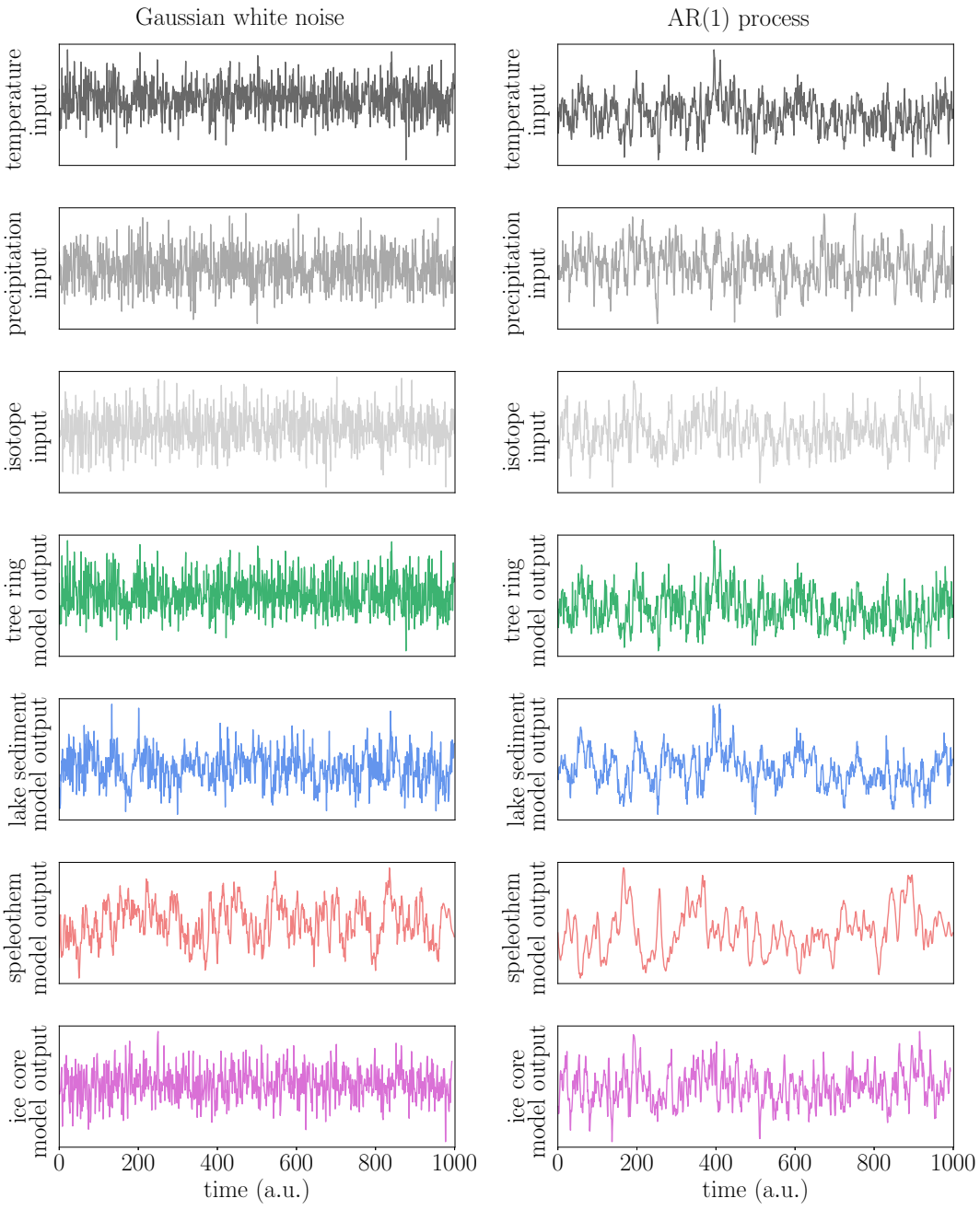

Figure S2. Annually resolved input time series for temperature, precipitation and isotopic composition and corresponding model output time series (top to bottom) for the two noise processes (left: Gaussian white noise, right: AR(1) process).

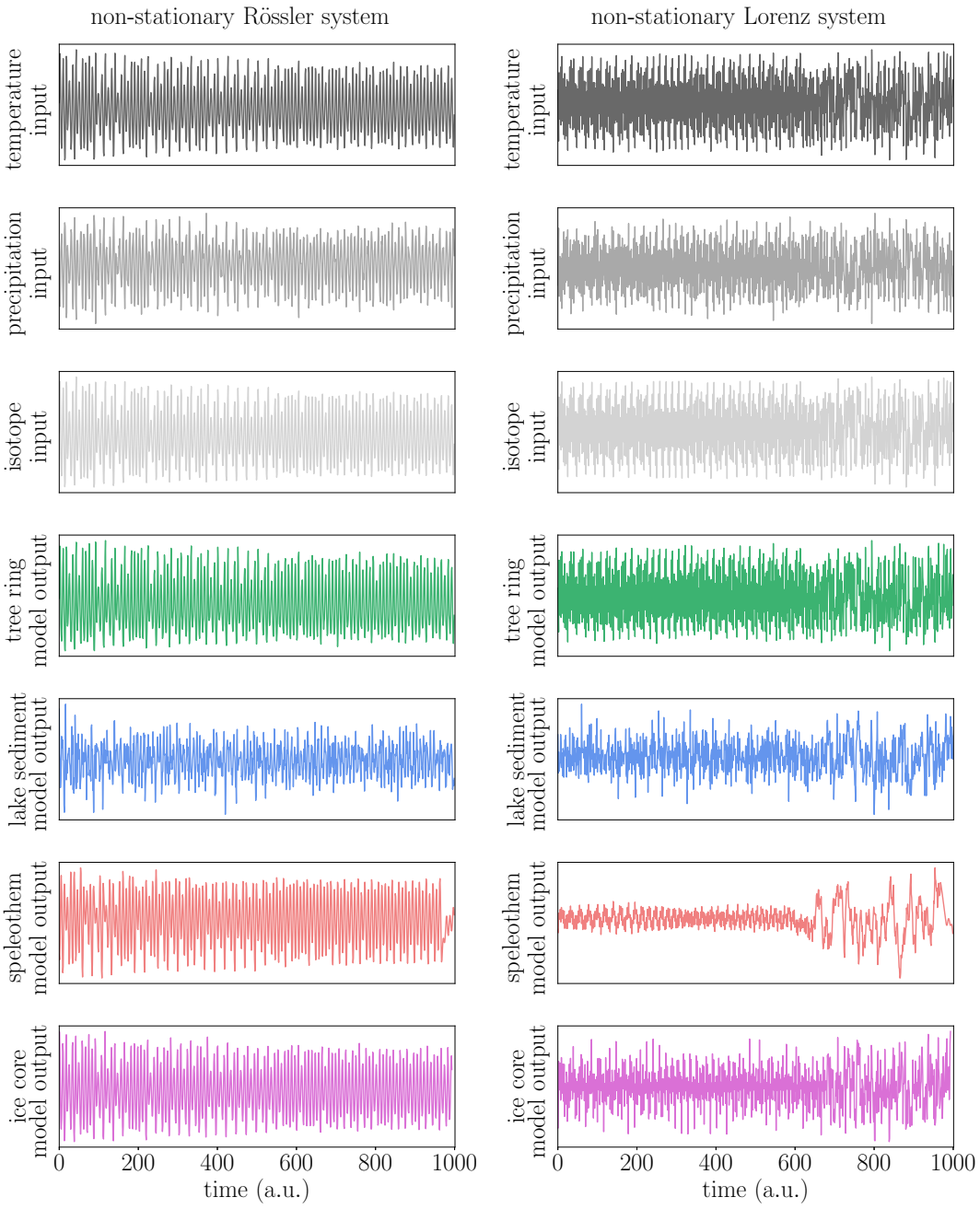

Figure S3. Same as in Fig. S2, but for the two deterministic non-stationary systems (left: non-stationary Rössler system, right: non-stationary Lorenz system).

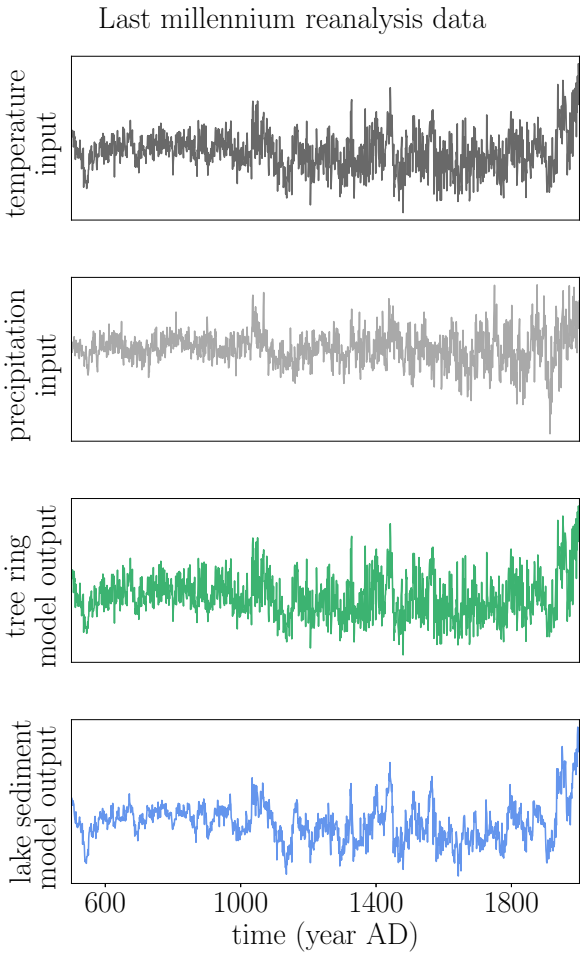

Figure S4. Annually resolved input time series for temperature and precipitation and corresponding model output time series (top to bottom) for the last millennium reanalysis data (Hakim et al., 2016; Tardif et al., 2019).

Time series properties

In order to complement the results of recurrence network analysis and better understand their possible dynamical meaning, we take a look at the properties of the time series generated by the different proxy system models and compare them to those of the input time series. Figures S2 to S4 display the annually sampled input time series for temperature, precipitation and isotopic compositions and the corresponding output time series of the four proxy system models for the five input scenarios of GWN, the AR(1) process, the non-stationary Rössler system, the non-stationary Lorenz system, and the last millennium reanalysis data. The expected low-pass filter effects of the speleothem, ice and lake models due to the cave residence time, diffusion, and bioturbation, respectively, are directly visible in the time series, while for the tree model, such an effect is neither expected nor visible. Also, it should be noted that the tree ring model with the parameters as specified in Table 1 seems to primarily respond to temperature rather than to precipitation, meaning that the limiting factor for tree growth in eastern Canada is temperature, which is ecologically reasonable and also be related to the fact that precipitation is only indirectly taken into account in the used model for tree ring width.

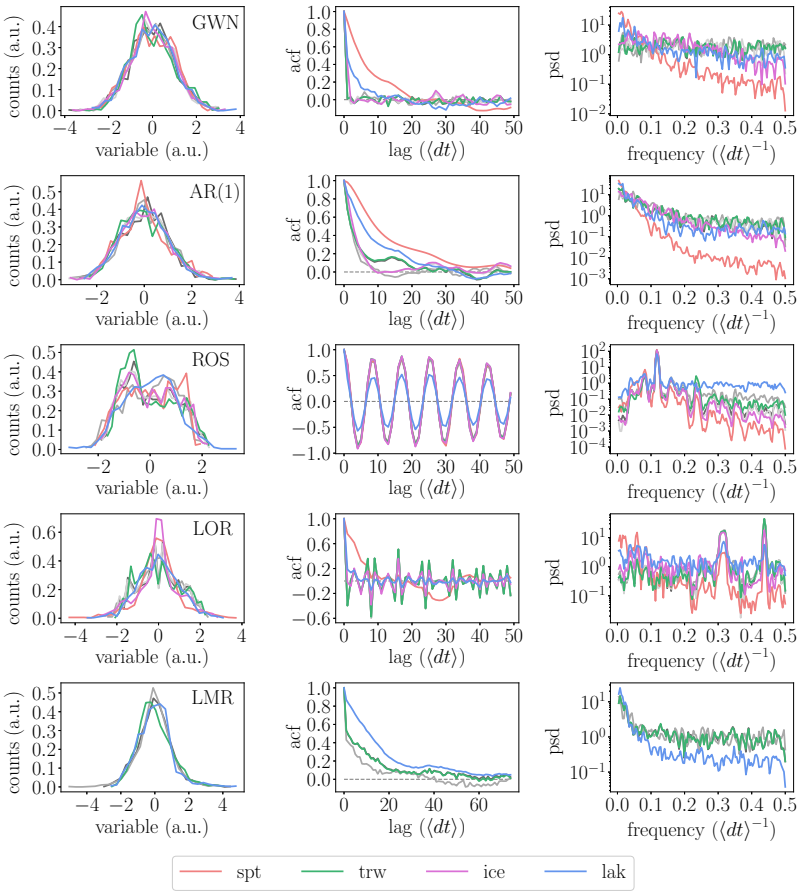

Figure S5. Normalised histograms, autocorrelation functions (acf) and estimated power spectral densities (psd) of the different input and proxy system model output time series for GWN, AR(1), ROS, LOR, and LMR (top to bottom). The input variables are denoted in grey, the tree model output in green, the lake model output in blue, the speleothem model output in red, and the ice model output in magenta.

For further evaluation, we standardise all time series to zero mean and unit variance and examine some properties of the different input and output series. The left panels of Fig. S5 show the normalised histograms of the input and output variables. To quantify differences in the histograms, we consider the skewness of the distributions of the different time series (see Table S1). We observe that the resulting time series from the tree model all show significant deviations in skewness from the input data, which is probably due to the thresholding of the growth response functions for temperature and soil moisture. For the other proxy models, we observe a significant influence of the model on the skewness of the output for those inputs that are not stochastic. This might either be related to the smaller confidence bounds due to the different surrogate generation, or hint to a different reaction of the models to different distributions of the input data.

Finally, we have a look at the autocorrelation functions and the power spectral densities of the different input and proxy model output time series. The middle and right panels of Fig. S5 show the resulting autocorrelation functions and estimates of the power spectral density obtained using the Welch method (Welch, 1967). As before, we observe that the autocorrelation function and power spectral density of the tree ring model output closely follow the respective temperature input. The good agreement between the temperature input and the tree ring width model output can be partially attributed to the model not taking into account juvenile growth of the trees. The speleothem model output shows the expected loss of power in the higher frequencies. Similarly, a loss of power in the higher frequencies can be observed in the ice core model output but not as

Table S1. Skewness of the different input and proxy system model output time series with significant deviations of the model output time series from the corresponding input marked in bold.

input/output	GWN	AR(1)	ROS	LOR	LMR
temperature	0.00	0.07	0.21	-0.02	0.33
precipitation	0.12	-0.03	-0.20	0.01	0.01
isotopes	-0.06	0.12	0.22	-0.02	–
trw	$\mathbf{0.34}$	$\mathbf{0.35}$	$\mathbf{0.40}$	$\mathbf{0.26}$	$\mathbf{0.63}$
lak	0.11	0.23	$\mathbf{-0.05}$	$\mathbf{0.01}$	$\mathbf{0.71}$
spt	-0.04	0.29	$\mathbf{-0.27}$	$\mathbf{0.26}$	–
ice	-0.01	0.15	$\mathbf{0.15}$	$\mathbf{-0.05}$	–

pronounced as for the speleothem model output. The same holds for the lake sediment model output except for the Rössler and Lorenz scenarios, where the lake model output shows more power in the higher frequencies than the corresponding input. This is most likely related to the different time-scales of variability present in those time series in comparison with the others and the particular choice of mixed layer thickness in the lake sediment model, $\mathrm{mxl} = 4$.

Skewness of time series

Table S1 gives the skewness of the distributions of the different time series where those values showing a significant deviation from the skewness of the corresponding input are marked in bold. To test whether the skewness values of the model output time series differ significantly from that of the respective input, we create $N_{\mathrm{sk}} = 10,000$ surrogate data sets for each of the input time series. For GWN and the AR(1) process, this is done by creating different realisations of the corresponding process according to the descriptions in Sec. 4, while for the other time series, the surrogates are created by adding white noise with signal-to-noise ratios of 25 for the model systems and 100 for the last millennium reanalysis data. Then, for each surrogate realisation, we calculate the skewness of the distribution and take the 0.5th and 99.5th percentile as confidence bounds resulting in the 99% confidence intervals of $[-0.20, 0.20]$ for GWN, $[-0.29, 0.29]$ for the AR(1) process, $[0.20, 0.23]$ for the non-stationary Rössler system, $[-0.03, 0.00]$ for the non-stationary Lorenz system, $[0.32, 0.34]$ for the last millennium reanalysis temperature, and $[0.00, 0.02]$ for the last millennium reanalysis precipitation. As precipitation is proportional to the negative temperature and isotopes, the corresponding confidence interval for the Rössler system is $[-0.23, -0.20]$ and for the Lorenz system $[0.00, 0.03]$.

References

Hakim, G. J., Emile-Geay, J., Steig, E. J., Noone, D., Anderson, D. M., Tardif, R., Steiger, N., and Perkins, W. A.: The last millennium climate reanalysis project: Framework and first results, Journal of Geophysical Research: Atmospheres, 121, 6745–6764, https://doi.org/10.1002/2016JD024751, 2016.

Tardif, R., Hakim, G. J., Perkins, W. A., Horlick, K. A., Erb, M. P., Emile-Geay, J., Anderson, D. M., Steig, E. J., and Noone, D.: Last Millennium Reanalysis with an expanded proxy database and seasonal proxy modeling, Climate of the Past, 15, 1251–1273, https://doi.org/10.5194/cp-15-1251-2019, 2019.

Welch, P.: The use of fast Fourier transform for the estimation of power spectra: A method based on time averaging over short, modified periodograms, IEEE Transactions on Audio and Electroacoustics, 15, 70–73, https://doi.org/10.1109/TAU.1967.1161901, 1967.